Renormalization Approach to Optimal Limiter Control in 1-D Chaotic Systems

C. Wagner[1] **and R. Stoop**[2]

Optimal limiter control of chaos in 1-d systems is described by flat-topped maps. When we study the properties of this control by a bifurcation analysis of the latter, we find partial universal behavior. The optimality of the control method is expressed by an exponentially fast control onto selected periodic orbits, making targeting algorithms idle.

Due to the wealth of unstable periodic trajectories of a chaotic attractor, the control (stabilization) of a system on these orbits offers an excellent tool for technical applications.[1–3] In the field of telecommunication, however, the calculation of the control signal needs to be done at a frequency in the GHz range, which requires a very fast and robust determination. Recently, Corron *et al.*[4] introduced a control method using simple limiters for which they claimed these properties. The simplicity of their control indeed drastically reduces the latency of the controller. Furthermore, in electronic circuits, the approach can easily be implemented using a diode, limiting the voltage (or current) if a given threshold is exceeded. As has been shown in ref. 5, the limiter control can be optimized, leading in the 1-d case to a description by the class of flat-topped maps. Beside the proposed use of the optimal limiter control scheme in telecommunication there is a variety of other applications. Glass and Zeng suggested its use in regularizing cardiac rhythms.[6] A chain of flat topped map was used by Sinha and Biswas to

---

[1] Institute of Pharmacology, University of Bern, Friedbuhlstr. 49, CH-3010 Bern, Switzerland; e-mail: clemens.wagner@pki.unibe.ch
[2] Institute of Neuroinformatics, University/ETH Zürich, Winterthurerstr. 190, CH-8057 Zürich, Switzerland.

investigate adaptive dynamics.[7] Moreover, Sinha and Ditto presented a simple network of flat topped logistic maps which encodes numbers and performs arithmetic computations.[8] The purpose of the present paper is to investigate to what extent the class of flat topped maps is associated with universal behavior.

Flat-topped unimodal maps cannot show chaotic motion, although they undergo a period doubling cascade, as a function of the height of the top. As a chaotic trajectory would explore the entire attractor of the system, it eventually will land on the flat segment, from which point onwards on it will continue on a periodic orbit. If we consider (nonergodic) maps having separated attractors, the periodic motion can only be observed if the orbit visits the attractor which is associated with the flat segment of the map. In the first step, we determine the properties of the bifurcation cascade and compare it with the Feigenbaum case. We will show that for flat-topped maps, the scaling for the opening of the forks is replaced by two different scaling factors. One of them is a trivial scaling by $\alpha = 1$, which is associated with the scaling of the top. The other scaling by $\tilde{\alpha}$ depends on the derivatives of the map and can therefore not be universal. For this splitting of scaling, we propose the term ''partial'' universality. In the course of period doubling, flat-topped maps show an exponential convergence towards the period-doubling accumulation point. As a consequence, the value of δ diverges. Of practical interest is the observation that the convergence onto the asymptotic periodic orbit is exponential and usually reached within a few iterations when starting from arbitrary initial conditions.

Flat-Topped Tent Maps. *Bifurcation cascade:* The flat-topped symmetric tent map is given by

$$x_{i+1} = \begin{cases} 1 - |2(x_i - 0.5)|, & \text{for} \quad 1 - |2(x_i - 0.5)| \leqslant h \\ h, & \text{otherwise,} \end{cases} \tag{1}$$

where the state variables at time $t = i$ and $t = i + 1$ are denoted by x_i and by x_{i+1}, respectively. The threshold h denotes our limiter, it also is the natural choice of the bifurcation parameter. Figure 1a, d shows the map and the bifurcation diagram, where the threshold h is increased from $h = 0.5$ to $h = 1$. For the diagram, the last 100 of a trajectory of 500 points are plotted, showing that the associated orbits are periodic, except for $h = 1$. Upon this increase of h, the length of the flat interval shrinks from $l_{h=0.5} = 0.5$ to $l_{h=1} = 0$. In Fig. 1d, for each h the interval end points are shown as thin lines. In the bifurcation diagram a period doubling bifurcation occurs whenever an end point collides with a 2^n-periodic fixed point.

Therefore, a new controlled orbit is born when the diagonal $x_{n+1} = x_n$ first hits a flat interval of the 2^n-fold iterated map. When h is further increased, the intersection point moves along the flat interval to the other end point, where the next period doubling bifurcation is generated. Because of the constant absolute slope of the map, all branches in the bifurcation diagram are straight lines. For an orbit of length 2^n, the slope of the bifurcation branch that contains $x = 0.5$ can be written as $s_n = 2^{2^{n-1}}$, $n > 0$. The sequence of period doubling bifurcation can now be calculated as the intersections of
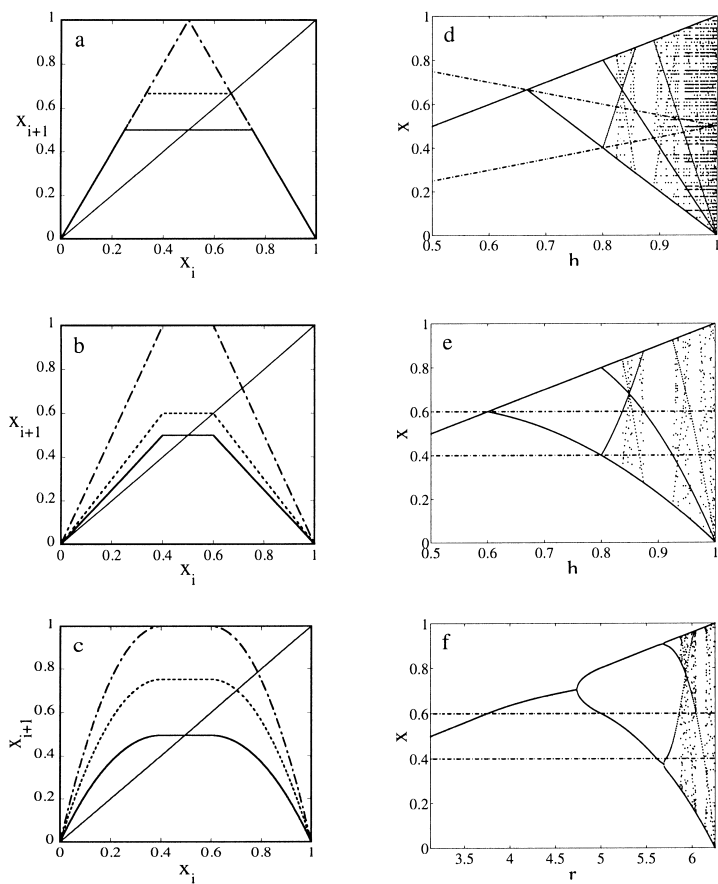

Fig. 1. (a) Flat-topped tent, (b) spread tent, (c) spread logistic map, with corresponding bifurcation diagrams (d–f).

this branch with the lines corresponding to the end points of the flat top. For $n > 1$ this leads to

$$h_n = 1 - \frac{\prod_{k=0}^{n-2} (2^{2^k} - 1)}{2^{2^{n-1}} + 1}, \tag{2}$$

where 2^n denotes the periodicity of the cycle. The location of the threshold at which the periodicity becomes infinite can numerically be determined as $h_\infty \sim 0.82490806728021$.

Scaling properties: The scaling behavior of 1-d unimodal maps is characterized by two constants α and δ. The constant α asymptotically describes the scaling of the fork opening by subsequent period doubling, whereas δ represents the scaling of the intervals of period 2^n to that of period 2^{n-1} near the period doubling accumulation point, i.e. at the transition to chaos. Both values depend on the order of the maximum of the map. The usual Feigenbaum constants correspond to the prominent class of maps with non-vanishing curvature at the hump. Therefore, it is not a surprise that for flat-topped maps, this scaling behavior is changed. The value of α can be determined from the fixed point of the period doubling operator T (e.g., ref. 9)

$$g(x) = Tg(x) = -\alpha g\left(g\left(-\frac{x}{\alpha} \right) \right), \tag{3}$$

where $g(x)$ denotes the fixed-point function. For the corresponding ansatz, we first study the renormalized function $g_{n,1}(x) = (-\alpha)^n f_{h_{n+1}}^{2^n} \left(\frac{x}{(-\alpha)^n} \right)$, at h_n, where 2^n denotes the periodicity of the orbit. The scaling function $g(x)$ then is obtained as $g(x) = \lim_{i \to \infty} \lim_{n \to \infty} g_{n,i}(x)$. The form of the rescaled functions $g_{n,1}(x)$ for $n = 0, 1, 2, 3$ motivates that $g(x)$ is a square wave. Therefore, we make the ansatz

$$g(x) = 1 + b(1 + \Theta(x-1) - \Theta(x+1)), \tag{4}$$

where $\Theta(x)$ represents the Heaviside function. Insertion of (4) into (3) leads to

$$1 + b(1 + \Theta(x-1) - \Theta(x+1))$$
$$= -\alpha\left(1 + b\left(1 + \Theta\left(g\left(-\frac{x}{\alpha} \right) - 1 \right) - \Theta\left(g\left(-\frac{x}{\alpha} \right) + 1 \right) \right) \right) \tag{5}$$

Fig. 2.   Split scaling of forks: The horizontal scaling ($\alpha = 1$) is universal. The vertical scaling ($\tilde{\alpha}$) depends on the derivatives of the map.

This equation allows for $\alpha = 1$ and $b = -2$ as solutions.[10] The value of $\alpha = 1$ implies that in the vicinity of the accumulation point h_∞, the opening of the bifurcation fork does not change under subsequent period doubling bifurcation. However, as the map has everywhere a non-zero slope of absolute value 2, the ratio of the fork openings within a 2^n periodic orbit is $\tilde{\alpha} = 2$.[11] This is illustrated in Fig. 2 which shows the location of the forks in the bifurcation diagram versus the periodicity of the orbit. Each circle represents a bifurcation fork, which openings can be calculated by multiplying all factors along the path, starting at the period 2 orbit. E.g., in order to calculate the opening size of the (from top) forth fork of period 16, we follow the bold path in Fig. 2 and obtain $1 \circ \tilde{\alpha}^{-1} \circ 1 \circ 1 \circ \tilde{\alpha}^{-4} = \tilde{\alpha}^{-5}$. Note, that the value of $\alpha = 1$ is only exact close to the accumulation point whereas the value of $\tilde{\alpha} = 2$ is always exact.

Instead of considering the bifurcation points h_n at which periods of order 2^n are born, the value of δ can be determined by using the values H_n where the periodic orbits contain the point $x_i = 0.5$, as both sequences converge with the same behavior to the accumulation point h_∞. The value of the bifurcation parameter H_n is given by

$$H_n = 1 - \frac{\prod_{k=0}^{n-1} (2^{2^k} - 1)}{2^{2^n}}. \tag{6}$$

Equation (6) can be written recursively as

$$H_n = 1 - (1 - H_{n+1}) \frac{1}{1 - 2^{-2^n}}, \tag{7}$$

which leads to

$$H_n = 1 - (1 - h_\infty) \prod_{k=n}^{\infty} \frac{1}{1 - 2^{-2^k}}. \tag{8}$$

Using $\prod_{k=n}^{\infty} (1 - 2^{-2^k})^{-1} \approx (1 - \sum_{k=n}^{\infty} 2^{-2^k})^{-1} \approx 1 + 2^{-2^n}$, Eq. (8) reduces to

$$H_n = h_\infty - c 2^{-2^n}, \tag{9}$$

where $c = 1 - h_\infty$. Equation (9) reveals an exponential convergence towards the fixed point. Therefore, the ratio between two subsequent intervals $H_n - h_\infty$ and $H_{n+1} - h_\infty$, which asymptotically determines the value of δ, depends on n as

$$\delta^{-1}(n) = 2^{-2^n}. \tag{10}$$

This result shows that in the case of the flat-topped tent map, the occurrence of period doubling does not follow a power law. Rather, it is of exponential nature.

Time needed to control: Unstable periodic orbits can only be controlled when the system is already in the vicinity of the orbit. As the initial transients can become very large, targeting algorithms have been designed[12, 13] that efficiently push the system onto the selected orbit. The flat-topped tent map and the corresponding tent map share the same orbit if the threshold of the flat-topped tent map coincides with the largest fixed point of the tent map. Due to the flat top, this orbit becomes stable. Initial conditions that lead to the flat top are on the selected orbit within one iteration. Iterating backwards, we can determine the intervals which lead to the orbit in two iterations, and so on. This approach is similar to the strange repeller escape problem. The relationship suggests that in our case, the convergence onto the selected orbit is exponential, which makes a targeting algorithm idle.

The exact convergence onto the selected orbit depends on the size of the flat top. The larger the horizontal segment is, the faster is the convergence. As the size of the flat top is determined by the threshold, the time constant of convergence varies with the latter. We calculated the time constant for h_∞ by propagating back the interval associated with the flat top. For each back-iteration, $2k$ new intervals of half the size of the intervals obtained by the previous step join the already recruited intervals. This

Table I.   Number of Back-Iterated Intervals

back iteration i	1	2	3	4	5	6	7	8	9	10	11	12
k	1	2	3	5	7	10	13	18	23	30	37	47
Δ		1	1	2	2	3	3	5	5	7	7	10	10

property is due to the slope of the map, which equals 2 in the present case. Table I gives the number of back-iterations versus half of the number of the added intervals k.

Let the differences between two subsequent values of k be denoted by $\Delta(i)$, where i denotes the order of the backward iteration. From their values, it is seen that k can be calculated iteratively as

$$k(i) = k(i-1) + \Delta(i-1), \tag{11}$$

where $i \geqslant 2$, $k(1) = 1$, $\Delta(1) = 1$, $\Delta(2i) = k(i)$ and $\Delta(2i-1) = k(i)$. The length L denotes the measure of naturally, i.e., equally distributed, initial conditions which do not lead to the selected orbit. The reduction of L due to i-fold back iteration can then be written recursively as

$$L(i+1) = L(i) - 2k(i)\frac{l_0}{2^i}, \tag{12}$$

where l_0 denotes the initial size of the flat top. If properly scaled, $1 - L(i)$ is the probability measure for initial conditions to be controlled onto the selected orbits in i steps. Figure 3a shows the convergence onto the orbit for $h = 2/3$, $h = h_\infty$ and $h = 0.85$ (full line, dashed line and broken line,
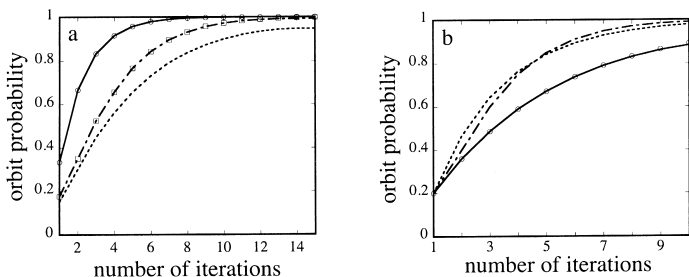

Fig. 3.   Convergence onto orbits versus steps. (a) Flat-topped tent map ($h = 0.85$, $h = h_\infty$, $h = 2/3$). Circles and squares from back-iteration [Eq. (12)] and from zeta function [Eq. (13)], respectively. (b) Spread tent map ($h = 1$, $h = 0.8$, $h = 0.6$). Circles: results from zeta function [Eq. (15)].

respectively). The squares represent calculations using Eq. (12). For the system to be controlled, it needs to visit the flat segment of the graph. The determination of the measure of orbits that reach the horizontal fragment after n iterations is equivalent to the escape problem of a (hyperbolic) strange repellor. Indeed, the average rates either for landing on the controlled orbit or for the escape is given by the decreasing number of chaotic orbits as a function of iterations. For the numerical treatment of hyperbolic repellors, one standard method is the cycle expansion.[14, 15] We used this approach to check our brute-force results for $h = 2/3$. The cycle expansion of the dynamical zeta function is then governed by the cycle that corresponds to the fixed point at $x = 0$ and reads

$$1/\zeta = 1 - z \tfrac{1}{2}. \tag{13}$$

The escape rate γ is determined by the zero of the dynamical ζ-function using $z = \exp(\gamma)$. This yields $\gamma = \ln(2)$, implying that for arbitrary initial conditions the probability of landing on the period 1-orbit within 5 iterations is $p = 0.95$.

Maps of Spread Type. A spread map is obtained from a fully developed chaotic map by separating the top of it and connecting the ends of the two branches with a horizontal line of the length $2d$. When varying the height of the map the horizontal segment remains constant. For the tent map this amounts to the equation

$$x_{n+1} = \begin{cases} \dfrac{h}{0.5-d}\, x_n, & \text{for} \quad x_n \leqslant 0.5-d \\[2mm] \dfrac{h}{0.5-d}\,(1-x_n), & \text{for} \quad x_n \geqslant 0.5+d \\[2mm] h, & \text{otherwise.} \end{cases} \tag{14}$$

Figure 1b shows the graphs for $d = 0.1$, at $h = 0.5$ (full line), $h = 0.75$ (broken line) and $h = 1$ (dashed line), as well as the bifurcation diagram using the height h of the map as bifurcation parameter (Fig. 1e). Since the flat top is symmetric about the line $x = 0.5$ and of constant size, the corresponding envelopes are two parallel horizontal lines at $0.5+d$ and $0.5-d$. Bifurcation can only occur at these two lines. The effect of the changed slopes of the map is reflected in the curved bifurcation branches shown in Fig. 1e, in comparison with the straight lines of the flat-topped tent map (Fig. 1d). Due to the dominance of the horizontal segment for the occurrence of bifurcations, the scaling by α remains unchanged. In contrast, the scaling by $\tilde{\alpha}$ changes from one period doubling to the next. Upon

a decrease of h, we observe two effects that influence the convergence onto the orbit. On the one hand, some of the orbits are lost, which reduces the number of intervals added by back-iteration. On the other hand, due to the decreased slope of the map, individual intervals becomes larger (except for the central one). The trade-off between these effects leads to an optimal convergence case at $h \approx 0.8$. Figure 3b shows the time constants obtained for decreasing heights ($h = 1$ (full line), $h = 0.8$ (dashed line) and $h = 0.6$ (broken line)), using $d = 0.1$. For $h = 1$, the exponential decay constant again can be calculated using the cycle expansion. The dynamical ζ function then is

$$1/\zeta = 1 - \frac{1}{1-2d}\, z, \tag{15}$$

which leads to $\gamma = \ln(1/(1-2d))$. In Fig. 3b, the calculated values are shown as circles.

The spread logistic map provides an example that is differentiable on the interval $[0, 1]$ (see Fig. 1c). The corresponding equations read

$$x_{i+1} = \begin{cases} rx_i(1-x_i-2d), & \text{for } x_i \leqslant 0.5-d \\ r(x_i-2d)(1-x_i), & \text{for } x_i \geqslant 0.5+d \\ r(0.5-d)^2 & \text{otherwise,} \end{cases} \tag{16}$$

where d again denotes half of the flat segment size, and r controls the opening of the underlying parabola. The height of the map is given by $h = r(0.5-d)^2$; this restricts the range of r to $0 < r \leqslant 1/(0.5-d)^2$. Figure 1f also shows the bifurcation diagram, using $d = 0.1$. Its shape differs greatly from those shown before and more resembles the ordinary period doubling bifurcation diagram of the logistic map. This is due to the smooth connections between the horizontal segment and the two branches of the map. Figures 4a and 4b illustrate the differing mechanisms at the first period doubling bifurcation for the flat-topped tent and the spread logistic maps. In the former case, the bifurcation abruptly emerges from the single flat segment of the second iteration. In contrast, the second iteration of the spread logistic map already has two different flat segments, and the bifurcation occurs along the smooth inter-segment connection. At the period doubling accumulation point these smooth transitions turn into step like transitions, conserving the scaling of $\alpha = 1$.

In conclusion, the simplicity of the optimal limiter control and the speed of convergence onto target orbits suggests a broad range of possible applications in engineering and biology. For flat-topped maps, the scaling
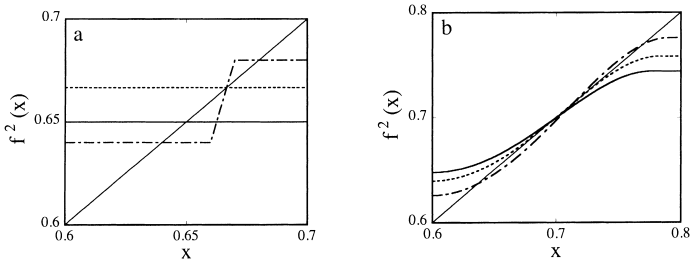
Fig. 4. Bifurcation mechanisms of flat-topped spread tent (*l*) and logistic maps (*r*). Second iteration maps before, at, and after bifurcations. Parameters: tent: $h = 0.65$, $h = 2/3$, $h = 0.68$, logistic: $r = 4.65$, $r = 4.74$, $r = 4.85$.

function $g(x)$ is a square wave with a scaling factor $\alpha = 1$ for subsequent period doubling bifurcation. The ratio of bifurcation fork openings within orbits of order 2^n depends on the derivative of the map and therefore does not follow a universal behavior. The scaling factor δ diverges. Close to the transition point, this kills the power law behavior for the occurrence of bifurcation, and an exponential law appears, which renders the observation of orbits of higher periodicity increasingly difficult. Although we already have shown that the limiter based control algorithm also works with the Henon map,[5] to what extent these properties are preserved in higher dimensions has still to be explored.

ACKNOWLEDGMENTS

REFERENCES

1. A. Garfinkel, M. Spano, W. Ditto, and J. Weiss, Controlling cardiac chaos, *Science* **257**:1230 (1992).
2. H. Schuster, *Handbook of Chaos Control* (Wiley–VCH, Weinheim, 1999).
3. I. Marino, E. Rosa, and C. Grebogi, Exploiting the natural redundancy of chaotic signals in communication systems, *Phys. Rev. Lett.* **85**:2629 (2000).
4. N. Corron, S. Pethel, and B. Hopper, Controlling chaos with simple limiters, *Phys. Rev. Lett.* **84**:3835 (2000).
5. C. Wagner and R. Stoop, Optimized chaos control with simple limiters, *Phys. Rev. E*, in press (2001).
6. L. Glass and W. Zeng, Bifurcations in flat-topped maps and the control of cardiac chaos, *Int. J. Bifurcation Chaos* **4**:1061 (1994).
7. S. Sinha and D. Biswas, Adaptive dynamics on a chaotic lattice, *Phys. Rev. Lett.* **71**:381 (1993).

8. S. Sinha and W. Ditto, Dynamics based computation, *Phys. Rev. Lett.* **81**:2156 (1998).

9. H. Schuster, *Deterministisches Chaos* (Wiley–VCH, Weinheim, 1994).

10. For $g(0) = 1$ one also could use the ansatz $g_n(x) = 1 + bx^{2n}$ and take the limit for $n \to \infty$. Again, the solution is a square wave with $b = -2$. Using $g(1) = -\alpha$ yields $\alpha = 1$ and $\delta^{-1} = 0$.

11. Scaling laws for "stars" and "windows" observed in the bifurcation diagram for $h > h_\infty$ of the logistic map were already described by Sinha.[16] They both depend on the derivative of the map at the origin and are therefore not universal. The scaling factor for "stars" and "windows" of the tent map is 2.

12. T. Shinbrot, E. Ott, C. Grebogi, and J. Yorke, Using chaos to direct trajectories to targets, *Phys. Rev. Lett.* **65**:3212 (1990).

13. E. Kostelich, C. Grebogi, E. Ott, and J. Yorke, Higher-dimensional targetting, *Phys. Rev. E* **47**:305 (1993).

14. R. Artuso, E. Aurell, and P. Cvitanovich, Recycling of strange sets: I. Cycle expansion, *Nonlinearity* **3**:325 (1990).

15. R. Artuso, E. Aurell, and P. Cvitanovich, Recycling of strange sets: II. Applications, *Nonlinearity* **3**:361 (1990).

16. S. Sinha, Unidirectional adaptive dynamics, *Phys. Rev. E* **49**:4832 (1994).